Time-resolved prompt-gamma activation analysis at spallation neutron sources and applications to cultural heritage, security, and radiation protection

Giovanni Romanelli [a], Giulia Festa [b,*], Dalila Onorati [c], Enrico Preziosi [c], Pierfrancesco Ulpiani [d], Carla Andreani [c], Roberto Senesi [c,e]

[a] *ISIS Facility, Rutherford Appleton Laboratory, Chilton, Didcot, Oxfordshire, OX11 OQX, UK*
[b] *Museo Storico Della Fisica e Centro Studi e Ricerche "Enrico Fermi", Piazza Del Viminale 1, Rome, 00184, Italy*
[c] *Università Degli Studi di Roma "Tor Vergata", Dipartimento di Fisica and NAST Centre, Via Della Ricerca Scientifica 1, Rome, 00133, Italy*
[d] *Università Degli Studi di Roma "Tor Vergata", Dipartimento di Scienze e Tecnologie Chimiche, Via Della Ricerca Scientifica 1, Rome, 00133, Italy*
[e] *CNR-IPCF Sezione di Messina, Viale Ferdinando Stagno D'Alcontres 37, Messina, 98158, Italy*

ARTICLE INFO

ABSTRACT

The present and future developments of time-resolved prompt-gamma activation analysis (T-PGAA) at pulsed neutron sources is discussed in the framework of the successful history of neutron-activation techniques. A brief description of the state of the art and the most important user facilities using standard prompt-gamma activation analysis (PGAA) is provided. Then, we discuss the challenges and the opportunities for T-PGAA at pulsed neutron sources, and the potential impact for applications to cultural heritage, radiation protection, and security. We notice some *inversions of trend* needed for the further development of T-PGAA with epithermal and fast neutrons, such as the possibility to use fast and high-efficiency γ-ray scintillators with lower energy resolution (compared to usual high-purity germanium detectors) when the signal from neutron capture resonance is selected. We also suggest how detection systems often used in other fields, such as medical physics, can be of interest and inspiration also in the case of neutron-based investigations. Finally, we present new data of T-PGAA measurements on VESUVIO using neutron energies up to the keV using the scintillators available on the instrument, for samples of gold (of interest in cultural heritage), cadmium (for environmental safety), and tantalum (a material used in biomedical implants).

1. Introduction

Already 15 years after the discovery of the neutron and artificial radioactivity, the analytical procedures for elemental analysis based on neutron activation were clearly established [1,2]. At first, the technique obtained increasing interest for the capability to discriminate rare-earth concentrations [3,4], a task much harder using chemical-separation techniques. Moreover, as the samples could be measured without any chemical preparation, the technique avoided contamination of the material prior to its characterization. For this reason, early articles referred to the neutron activation technique as *instrumental* [5], as opposed to other techniques involving chemical separation. In the following years, neutron activation analysis was employed to tackle a variety of problems, *e.g.,* detecting traces of toxic compounds to protect the environment [6,

7], or obtaining the elemental composition of human body samples [8] as well as *in vivo* [9]. Amongst the earliest studies, neutron activation analysis found an important application in the field of cultural heritage, with pioneering applications to ancient Mediterranean [10] and Roman [11] potsherds (the latter at Bepo at Harwell, UK). Over the past 20 years, a large interest in applying neutron techniques to cultural heritage investigations was expressed, *e.g.,* by the International Atomic Energy Agency [12] and through the Ancient Charm project [13,14]. As an example, the detection of corrosion compounds, such as copper chlorides, below the gilded bronze surface of the doors of the Baptistery in Florence, following the flood of Arno river in 1966, was presented in Ref. [15]. The results presented by those Authors clearly revealed the presence of chlorine in the unpolished surface of the bronze artefact, as opposed to the region treated with the traditional method of the Rochelle

---

* Corresponding author.
  E-mail address: giulia.festa@cref.it (G. Festa).

salts (see Fig. 1, further discussed later). Other recent examples of traditional neutron activation techniques include the investigation of Egyptian artefacts [16–18] and chipped stone tools [19]. The application of PGAA to cultural heritage and other topics has been reviewed in a number of publications, *e.g.*, Refs. [20–23].

Neutron activation techniques are based on the transformation of a stable isotope of an element, upon bombardment of neutrons, into a radioactive one, and measuring the decaying products. These can be either prompt γ-rays, following a nuclear de-excitation within few femtoseconds after the capture of the neutron by the mother isotope, or delayed γ-rays, possibly following a β decay to the daughter isotope. In the former case, one talks of Prompt Gamma Activation Analysis [8,24, 25], PGAA, while in the latter case one refers to the technique as Neutron Activation Analysis, NAA, or Instrumental NAA, INAA. The two techniques allow the detection of different elements in a given sample and, therefore, provide complementary pieces of information. For instance, PGAA is more suitable to detect the amount of light-weight elements like hydrogen and carbon in materials, while NAA allows very precise determination of heavy-weight elements, such as rare-earth isotopes. Finally, there are elements like gold, silver, and copper, of particular interest in cultural-heritage investigations, that can be detected, in principle, by both techniques. In PGAA, when the energy of the decaying γ-ray is completely released within a detector, a peak can be observed (generally referred to as full-energy peak) that is a fingerprint of the isotope that captured the irradiation neutron. Looking again at Fig. 1 as an example, the two prompt γ-rays from ^{35}Cl, at 788.4 keV and 517.1 keV [25], are pictorially labelled in the PGAA spectra from Ref. [15]. Despite being the two most-intense prompt γ-ray lines of chlorine in this energy region, they are barely detectable in the experimental spectra shown because of the little amount of chlorine compounds underneath the artefact surface, yet enough to deteriorate it if not carefully cleaned.

Both PGAA and NAA were employed, historically, taking advantage of cold and thermal neutron beams at continuous sources, with the capture reaction being driven by the absorption cross section, proportional to the inverse of the neutron velocity. More recently, the advent of spallation neutron sources allowed the use of epithermal neutron beams in the energy range 1 eV–1 keV. In this region, several elements, particularly of interest for cultural heritage, display intense and narrow peaks in the neutron cross section driven by resonant capture processes. An example is provided in Fig. 2, where the capture cross sections of natural copper, tin, and chlorine [26] are shown in the neutron energy range between 1 meV and 1 keV, with the vertical dashed line corresponding to the reference thermal neutron energy of 25.3 meV.

Moreover, as opposed to what happens at continuous neutron sources, pulsed spallation neutron facilities using the Time-Of-Flight (TOF)
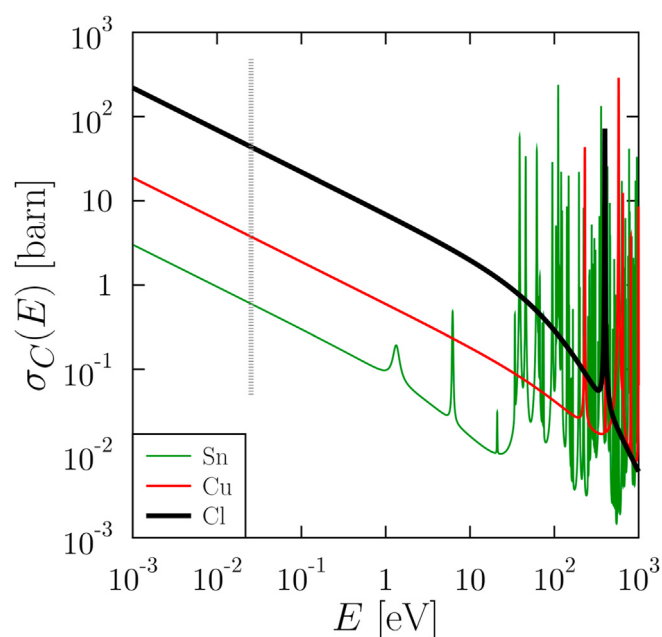
Fig. 2. Capture cross section of natural copper, tin, and chlorine from the ENDF-VIIIb library [26].

technique, allow to collect spectra where the signal from epithermal neutron resonances can be separated and analysed independently. In particular, if an instrument is equipped with a γ-ray detector, by collecting the neutron-induced prompt γ-rays from a sample, one can use the technique generally referred to as Neutron Resonance Capture Analysis, NRCA [27]. In this article, we describe some recent developments in combining the two techniques of PGAA and NRCA, thus measuring, for a given sample, the prompt γ-rays emitted as a function of both the energy of the neutron resonantly captured, and the energy of the γ-ray [28]. This technique is referred to as Time-resolved PGAA, or T-PGAA [29]. Moreover, we summarise the requirements of future instruments where T-PGAA can be concurrently applied to other neutron techniques, and we suggest some possible applications including cultural heritage, security, and radiation protection investigations.

2. The state of the art

Neutron activation techniques require two main ingredients: a neutron source for the irradiation and activation of a given sample, and
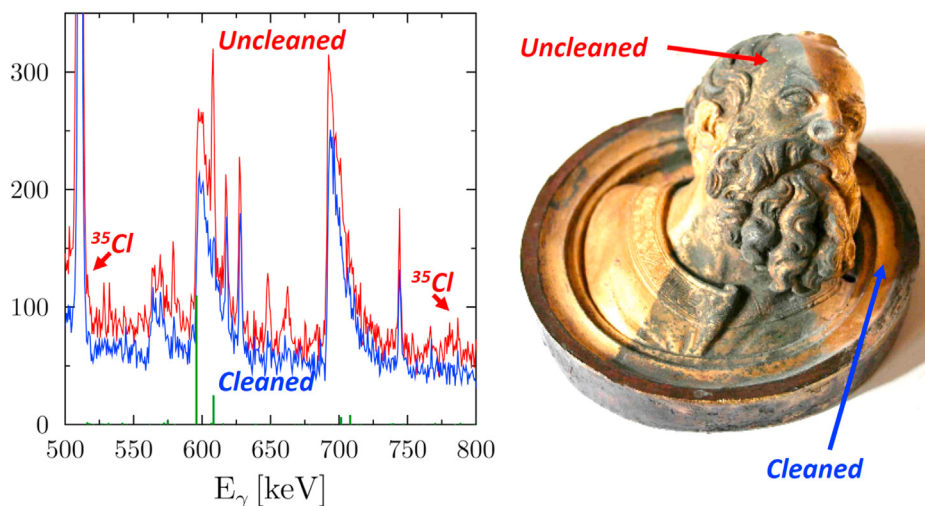
Fig. 1. Traditional PGAA spectra (left, arbitrary units) from two different regions of the bronze artefact (right) from the Baptistery of Florence. In particular, the uncleaned region (red) and the one cleaned using the Rochelle salts (blue) are shown. Data are adapted from Ref. [15]. In particular, the prompt-gamma lines from ^{35}Cl at 788.428 keV and 517.073 keV, discussed later, are marked with red arrows. Also, the prompt γ-rays from Ge isotopes [25], discussed in Sec. 2.3, are reported as green pulses with intensities in units of 10^{-2} b. (For interpretation of the references to colour in this figure legend, the reader is referred to the Web version of this article.)

the detection equipment and environment to measure the decaying γ-rays. Moreover, following the increasing use of PGAA in recent decades, more attention has been paid to the design of dedicated sample environment and low-background blockhouses. These components are briefly summarised in the following paragraphs.

2.1. Neutron sources

Very first examples of experiments based on neutron activation include the bombardment of Be targets with deuterium accelerated in a cyclotron [4] or Van de Graaf accelerators [30]. Starting from the 1952, an open service for industrial and academic users was available at the graphite-uranium nuclear reactor of the Oak Ridge National Laboratory [31], as a "new service to analysts". At the same time, attempts were also made to export this methodology, using natural neutron sources, into commercial and industrial laboratories [32]. These initiatives suggested the high potential impact of neutron-irradiation techniques for a variety of uses, both industrial and academic.

The first examples of dedicated user facilities for PGAA studies include the NIST Centre for Neutron Research [24,42,43] using both cold and thermal neutron beams in the 1990', quickly followed by facilities at Julich [33], Budapest [35], Tokai [34] and FRM-II [36,44]. Cold neutrons are often preferred to thermal ones because the absorption cross section $\sigma_a(E)$ has an inverse dependence upon the incident neutron energy E, of the form [45].

$$\sigma_a(E) = \sigma_a(E_0)\sqrt{\frac{E_0}{E}}, \tag{1}$$

with $E_0 = 25.3$ meV and the parameter $\sigma_a(E_0)$ available in standard libraries such as Ref. [46]. For this reason, cold neutrons provide a higher capture rate than thermal neutrons, thus a larger decaying signal.

While reactor-based facilities, using cold and thermal neutrons, are generally continuous sources, the advent of accelerator-driven spallation neutron sources provided two novel opportunities. First, when slowing down fast neutrons generated in a spallation process, a significant flux of under-moderated epithermal neutrons is available. This is evident from Fig. 3, where we report the neutron flux at the sample position of the VESUVIO instrument at the ISIS spallation source (UK). Epithermal
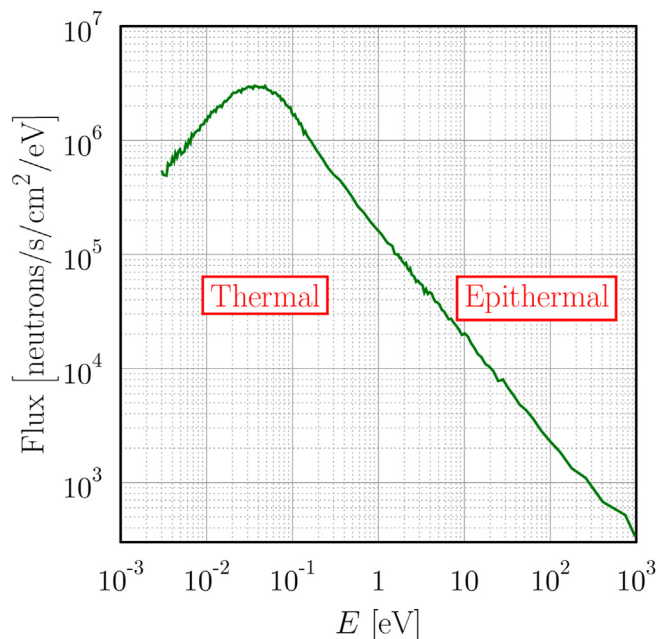

Fig. 3. The neutron beam flux at the sample position of the VESUVIO spectrometer at ISIS. Data adapted from Ref. [47].

neutrons have an additional probability to be captured by a given nucleus and emitting a γ-ray, through Breit-Wigner-like resonances of the form [27]:

$$\sigma_\gamma(E) = \frac{h^2}{8\pi m_N E}\sum_\mu g_\mu \frac{\Gamma_n \Gamma_\gamma}{(E-E_\mu)^2 + \Gamma^2/4}, \tag{2}$$

with E_μ the central energy of the μ-th resonance, g_μ the related multiplicity factor, the parameters Γ_n and Γ_γ are the full width at half maximum related to the probability of capturing a neutron and emitting a photon, respectively, and $\Gamma = \Gamma_n + \Gamma_\gamma$. Finally, h is the Plank's constant and m_N the neutron mass. As already shown in Fig. 2, these resonances provide intense and well-localised peaks in the capture cross section, and their positions are "fingerprints" of different isotopes.

The second opportunity at spallation sources is that their pulsed nature allows TOF measurements whereby the time t when a neutron is captured by the sample at a given distance L_0 from the neutron moderator is related to the time t_0 when the spallation process takes place in the source via the neutron energy as

$$t - t_0 = \sqrt{\frac{m_N}{2E}}L_0. \tag{3}$$

One should notice that neutron choppers can be used to transform a continuous thermal or cold neutron beam into a pulsed one, as one can appreciate in the case of PGAA studies using pulsed cold neutron beams at NIST [48] and Budapest [49]. However, their effectiveness for epithermal neutrons quickly worsens with the increasing neutron energy. Some examples of neutron energy selection using choppers are provided in Refs. [50,51].

Table 1 reports a list of neutron instruments and facilities where PGAA is available at present for users, also mentioning if the neutron source is operated in a continuous or pulsed way. Ref. [20] reports a longer list of facilities operating in the periods 1966–2000. A more recent review, with particular attention to compact neutron sources, was presented in Ref. [52]. It is also worth noting that, in a 2015 list of PGAA instruments and facilities provided by one of the IAEA working groups [53], only the ANNRI instrument at J-PARC [40] was mentioned amongst the spallation sources, although its main application is aimed to the determination of capture cross sections for nuclear databases [54]. One can notice how reactor sources generally provide neutron beams that are continuous in nature, while spallation sources provide pulsed neutron beams. Two important exceptions are presented by the SINQ continuous spallation facility [37], and the reactor at the Frank Laboratory of Neutron Physics at Dubna working as a pulsed source [38]. It is also worth noting that, in the latter case, epithermal neutrons are used at the Regata instrument to enhance the NAA signal from some trace elements. Finally, PGAA capabilities are also reported at the Centro Atomico Bariloche (CAB), where a Linear Accelerator (LINAC) is used to accelerate electrons and obtain a pulsed source of fast neutrons following the interaction of bremsstrahlung photons on a target [39].

Table 1
Some examples of instruments and user facilities where PGAA is available, underlining the distinction between continuous (cont.) or pulsed sources.

Instrument; Facility	Source	Ref.
CN/TN-PGAA; NIST	Reactor (cont.)	[24]
ELLA; KFA, Julich	Reactor (cont.)	[33]
JAERI; Tokai	Reactor (cont.)	[34]
PGAA/NIPS; Budapest	Reactor (cont.)	[35]
FRM-II; MLZ	Reactor (cont.)	[36]
PGA; SINQ, PSI	Spallation (cont.)	[37]
REGATA; FLNP, Dubna	Reactor (pulsed)	[38]
CNAB; Bariloche	LINAC (pulsed)	[39]
ANNRI; J-PARC	Spallation (pulsed)	[40]
INES; ISIS	Spallation (pulsed)	[29]
VESUVIO; ISIS	Spallation (pulsed)	[41]

2.2. Neutron guides and blockhouses

Early applications of PGAA explored the possibility to perform the experiment either placing the sample within a reactor [55] or outside [8], irradiating it through a beam port. The main advantages in having the sample within the reactor, *i.e.*, the high neutron flux bombarding the material under investigation, was completely overcome by the advent of neutron guides, as discussed in the next paragraph. However, it is interesting to notice that at pulsed neutron sources, where the TOF technique is employed, the resolution on the incident neutron energy improves with increasing primary flight length, L_0, between the source and the sample position, as one can appreciate from Eq. (3). Therefore, the development of T-PGAA requires the choice of a suitable value of L_0, long enough to provide a reasonable neutron-energy resolution between epithermal neutron energies, yet not too long so as to provide a decent neutron flux at the sample position.

Neutron guides are generally used for thermal and cold sources. In fact, neutrons with wavelengths larger than ca. 1 Å can be redirected towards the sample position following a full reflection on a properly treated and polished guide wall. Neutron guides allow, amongst other advantages, to obtain a high-intensity and uniform beam profile at the sample position. Moreover, curved guides can be used to separate cold and thermal neutrons from the epithermal-neutron component as well as γ-rays from the neutron source contributing to the background in standard PGAA measurements. On the other hand, neutron guides are not efficient for epithermal neutrons, for the particle's wavelength is shorter than any interatomic distance of the coating material, not allowing an efficient redirection of the neutron. For this reason, higher backgrounds are generally present at epithermal-neutron instruments, mainly related to the γ-rays generated within the target and moderator. For the same reason, the epithermal flux at the sample position cannot be boosted using a guide, as opposed to what happens for thermal and cold neutrons where typical gains are of the order of 10–100 (see, *e.g.*, Refs. [49,56]).

For the reasons mentioned above, PGAA experiments at spallation neutron sources require additional background characterization [57–59]. However, some tricks can be applied to all instrument blockhouses. For example, at NIST the sample environment is developed with hydrogen-free materials, so as to minimise the background for quantitative determination of hydrogen in samples using the 2223 keV prompt γ-ray emission line. In some cases, boron-free materials are used to avoid the emission of the prompt γ-rays at 478 keV following the neutron capture or, if not possible, additional layers of pure lead are used to absorb them. When neutrons need to be captured, ^{6}Li or equivalent absorbing materials are used, for example in the beam stop to avoid neutrons bouncing back into the blockhouse. Finally, the environmental radiation from scattered neutrons captured by the blockhouse walls can be minimised by, when possible, increasing the dimensions of the room and, more easily, by coating construction materials and walls with LiF tiles, as in the case of JAERI [34] and NIST [42].

It is worth mentioning the direct comparison of standard PGAA capabilities using thermal neutrons at the Rotax spectrometer at ISIS and at the Budapest reactor presented in Ref. [60]. The comparison was clearly favourable in the case of the reactor source for two main reasons. Firstly, reactor sources do not suffer from additional backgrounds from epithermal and fast neutrons. Secondly, and most importantly in our opinion, reactor sources have been investing on dedicated PGAA instruments for a number of years, while, at pulsed spallation sources, one has witnessed only a limited number of investigations on beamlines generally designed for other applications. However, again in Ref. [60] it was noted that the possibility to provide concurrent measurements using PGAA and other neutron techniques corresponded to an exciting scenario that, in our mind, needs the further development and use of T-PGAA, as opposed to standard PGAA, to succeed and become a concrete reality. This point will be further discussed later.

2.3. γ-ray detectors

Some early procedures, especially with low-intensity neutron sources [32] used Geiger-Muller flow counters, thus measuring the overall decay of the induced radioactivity of the sample, mainly related to the β-ray emission, rather than the energy spectrum of γ-rays. In those experiments and laboratories where the γ-ray energy was detected, first set-ups were equipped with fast NaI scintillator detectors. However, as these detector have a poor resolution of photon energies, one often needed to perform some chemical-separation processing of the irradiated sample so as to allow the interpretation of the collected spectra. This obstacle was overcome with the advent of Ge-based detectors [6], as they manifest a higher energy resolution, allowing the interpretation of spectra where the peaks from many isotopes are present at the same time.

In order to obtain good-quality PGAA spectra of the sample, it is important to keep the radiation background as low as possible, and one should have the capability to reject signals arising from incomplete energy deposition of γ-rays from the sample within the detector. In the latter case, γ-rays undergoing Compton scattering in the detector deposit only a variable fraction of their total energy, producing an undesirable continuum in the spectrum, worsening the detector sensitivity to full-energy peaks and the signal-to-noise ratio. For this reason, PGAA detection systems are often equipped with Compton suppression components. The usual approach is to surround the main detection unit dedicated to high resolution γ-ray spectroscopy, generally High-Purity Ge (HPGe) detectors, with an annular or quasi-annular Compton-suppression unit based on an array of high-efficiency scintillation crystal, often Bismuth Germanate ($Bi_4Ge_3O_{12}$, commonly referred as BGO), coupled to Photomultiplier Tubes (PMT). Different variations on this geometry are reported in the literature: a hollow cylinder of BGO surrounding the semiconductor detector [36,37]; a similar geometry but with an additional detection element to avoid additional background from backscattered γ-rays [14,61]; other designs in which the HPGe detector is not coaxial but perpendicular to the suppression system [43]; or PGAA detectors combining both the first and the latter configurations [36,37]. In these Compton suppressed detectors, the BGO components surrounding the HPGe detector operate in anti-coincidence mode, meaning that if a γ-ray interacting with the HPGe detectors undergoes Compton scattering inside it and then interacts in the BGO detector within a specified time window, the event is rejected. The opposite is also valid: γ-rays interacting in the suppression system and then revealed by the high-resolution detector will be rejected as well. In this way, unwanted signals, not contributing to a full-energy peak but providing a continuous background, will be rejected, thus improving the peak-to-background ratio and allowing a better sensitivity.

It is worth noting that anti-coincidence with BGO is only based on the occurrence of events in the same time window, but the BGO detectors are not used for Pulse-Height Analysis (PHA), for which they are not adequate due to their low light yield and slow decay time, at least compared with other scintillators. In fact, BGO is mainly used in these systems due to its high stopping-power and its low sensibility to neutron activation and capture. At the same time, HPGe detectors have low stopping-power compared to scintillation crystals and they need a cooling system and particular electronics. For this reason, designs in which the HPGe is replaced with scintillation crystal can be found in the literature [62]. We also note that some modifications of the HPGe-BGO standard design could provide additional benefit to the detection system. For example, the HPGe could be replaced with higher-efficiency and high light-yield scintillators (*e.g.*, LaBr$_3$). Replacing the BGO in the surrounding detectors with higher light-yield and faster decay-time scintillation crystals (*e.g.*, LYSO) could allow to make PHA also in the suppression detector, recovering events that deposit the overall energy between the spectrometer and the guard detector or to shrink the time windows for better Compton rejection, respectively. Table 2 provides a list of scintillation materials and their main properties, that could be of interest for future developments of T-PGAA, as discussed later.

Table 2
Comparison between HPGe, CZT and scintillation materials in terms of main properties. Data retrieved and averaged among multiple sources [63] and manufacturers' sites.

Detector	Z_{eff}	Density [g/cm^3]	Light Yield [ph/keV]	Energy Resolution [@ 662 keV]	Decay time [ns]
HPGe	32	5.36	–	–	–
CZT	42	5.78	–	–	–
LaBr3	45	5.08	71.6	2.8	22
CeBr3	45	5.18	58.0	3.2	20
SrI2	48	4.59	101.0	2.9	498
NaI(Tl)	51	3.67	44.2	6.3	240
LuYAP	60	7.2	10.0	7.9	30
LYSO	64	7.1	34.0	8.5	41
BGO	74	7.12	8.3	8.0	300

It is interesting to note how some of the peaks in PGAA spectra could be related to prompt γ-rays generated by neutrons scattered by the sample towards the detector and captured by elements within the detector. Some of these elements, *e.g.*, germanium in HPGe detectors, can participate with several lines to the background in a PGAA measurement. In the γ-ray energy range in Fig. 1 the main lines from a neutron capture correspond to the ^{73}Ge (n,γ)^{74}Ge prompt emissions at 595.9 keV and 608.3 keV, while the main lines from an inelastic scattering correspond to the reactions ^{74}Ge (n,n'γ)^{74}Ge at 595.9 keV and to ^{72}Ge (n,n'γ)^{72}Ge at 693.0 keV [25]. The PGAA lines from all the isotopes of Ge are reported in Fig. 1 and green pulses (with intensities in units of 10^{-2} b).

Regarding the design of the Compton suppression system, it is important to stress that Compton scattering cross section depends both on energy of the incoming γ-rays and the effective atomic number of the detector. For this reason, depending on the range of energies of interest, different choices could be made for the scintillation crystals. Moreover, the scattering angle strictly depends on the energy, following the Klein-Nishina formula, with forward scattering characterizing photons with energies above 1 MeV [64]. Again, depending on the range of energies of interest, the design of the suppression system could be optimized, as also discussed in Ref. [65].

As a final remark, since the choices related to geometry of both the primary detector and the shielding detector determine the performance in terms of sensitivity and background rejection, one should note that Monte Carlo simulations are fundamental for the optimization of the design of the overall detection system. Different simulations tools like MCNP [66,67], Geant4 [68–70] and FLUKA [71,72] have been used. It is important to stress that, especially in the production of prompt γ-rays, the most suitable Monte Carlo code and its libraries must be thoroughly selected, since evident differences in γ-rays yield are reported in the literature [73].

2.4. Detection methods from other fields of research

Prompt γ-ray detection is also of interest in other fields of research such as Medical Physics, especially for hadrontherapy [74,75], and environmental applications bib76[65,76]. In hadrontherapy, the prompt γ-rays, produced by protons and light ions used for radiotherapy, are fundamental to infer the range of the particles and the dose deposition inside the patient. Many solutions come from this sector, mainly focused on imaging but also focused on spectrometry, with several different designs that can be divided in four groups:

- Prompt γ-ray Imaging: by means of passive collimation through specifically designed components (*e.g.*, pinhole or knife-edge collimators) and position-sensitive detectors, the position from which prompt γ-rays is generated in the sample can be reconstructed [77,78];
- Compton Camera: using electronic collimation taking advantage of the energy deposition due to Compton interactions in subsequent

detectors and the angle between the interactions themselves, it is possible to reconstruct the position of the incoming γ-rays [79,80];
- Prompt γ-ray Timing: taking into account the time between the generation of the particle and the arrival of the γ-ray in the detector, it is possible to reconstruct the hadron transit time which can be correlated with the position of interaction inside the body of the patient from which the γ-ray was emitted [79,81];
- Prompt γ-ray Spectroscopy: is mainly devoted to reconstruct the composition of the interaction volume in the target depending on the different ratios of carbon and oxygen (from their specific lines in the spectrum) and it is possible to infer the type of tissue in which the interaction occurred [78,82–84].

Range verification could also be of interest in cultural heritage in the case of non-homogeneous artefacts. In addition to position detection, these approaches can suggest different geometries of detection suitable for T-PGAA experiments.

3. Development of time-resolved PGAA

Given the above discussion, the development of T-PGAA at spallation neutron sources represents an exciting opportunity as well as a challenging project. In this section, we will first review some past benchmark tests of T-PGAA investigations, then we will show some new T-PGAA data collected on the VESUVIO spectrometer at ISIS, and finally we will propose some suggestions for the further development of the technique over the coming years, *e.g.,* in the framework of a future ISIS-II facility [85].

3.1. Benchmark tests

Over the last decade, a number of experimental investigations were performed at ISIS for the development of instrumentation for epithermal neutron spectrometers [86], which combined the TOF technique with the detection of γ-ray emission spectra. In particular, in the case of the VESUVIO spectrometer [47], T-PGAA based acquisition set-ups were used for the development of the resonance-detector technique [87,88] in the case of YAP scintillators bib89[41,89] and CdZnTe detectors [90].

Over the past 5 years, T-PGAA has been used as a self-standing technique [28,29]. In particular, Toh et al. [28] applied the concurrent measurement of PGAA and NRCA at the ANNRI instrument at J-PARC. They explicitly noted how the two techniques require relatively different detector systems. On the one hand, NRCA using the TOF technique requires fast scintillators with generally lower γ-ray energy resolution. On the other hand, PGAA requires high-resolution (generally Ge) detectors, yet slow in nature. The Authors presented T-PGAA spectra from an array of HPGe detectors combined in anti-coincidence for background suppression. Shortly after, Festa et al. [29] showed the increase in elemental sensitivity of T-PGAA over standard PGAA at the INES spectrometer [91] at ISIS on a bronze standard. It was noted that a combined detection of both TOF and γ-ray energy provided a twofold advantage. On the one side, by analysing the PGAA spectra corresponding to the resonance energy of a given isotope, one could reduce the interference of γ-ray contributions at similar energies but from different elements. This was observed, for example, in the case of the γ-ray lines at ca. 163 keV from ^{107}Ag and ^{121}Sb, both typical trace elements in bronze, yet with the latter also often present in Pb shielding blocks. On the other hand, the T-PGAA acquisition also provided an advantage for NRCA, for the relative intensities of neighbouring resonances from different elements could be tuned by analysing the most advantageous portion of the biparametric (E_n, E_γ) plane. More recently [92], such apparatus and data treatment were upgraded in such a way to provide a quantitative analysis of the elemental composition of Cu-based certified standards, in preparation for applications to further cultural heritage investigations. This work provided an exquisite example of how neutron techniques can provide quantitative and accurate information in relation to bulk samples, whereas techniques such as X-ray fluorescence would be mainly sensitive

to the surface of materials investigated. Finally, PGAA experiments on [115]In making use of epithermal neutrons were reported by Granada et al. [39] at the CNAB facility. In particular, after positioning a thick cadmium foil between the neutron moderator and the sample, thus having the latter only irradiated with epithermal neutrons, the PGAA electronics was set-up so as to have the acquisition gate coinciding with the TOF of a given capture resonance of indium.

Recent investigations using T-PGAA at the VESUVIO beamline at ISIS where presented in Ref. [93] in the case of ancient Roman coins. VESUVIO has developed over the last decade from an instrument dedicated mainly to the measurement of nuclear quantum effects in materials [94], to an Epithermal and Thermal Neutron Analysis (ETNA) station [95,96] where the hydrogen quantitation using deep inelastic neutron scattering [97], neutron diffraction [47], NRCA [98] and energy-selective neutron transmission [99] can be applied at the same time on a given sample. In this framework, by mitigating the limitations at pulsed neutron sources already mentioned above [60], the addition of routinely available T-PGAA capabilities at the instrument will be an important addition.

3.2. T-PGAA on VESUVIO

In order to provide some examples of the T-PGAA capabilities at the VESUVIO instrument, we present below some newly collected spectra from samples of cadmium and tantalum, two materials of interest for a number of applications. In particular, cadmium is a pollutant material whose release in the environment can be toxic for life, and its quantitative detection represents a challenging and timely task [100]. Tantalum, on the other hand, is considered not to react with body fluids and, for this reason it is used in orthopaedic for manufacturing in hip and knee replacements, amongst other medical applications [101].

T-PGAA spectra were acquired using the same YAP detector and electronics previously employed in Refs. [102,103]. For each event detected by the YAP scintillator, a CAEN DT5730 digitizer was used to record the pulse height of the signal as well as the time stamp. The latter was combined together with the timing of the ISIS synchrotron so as to reconstruct the neutron TOF corresponding that event, and the TOF was then converted to the neutron energy. Fig. 4 shows the T-PGAA spectra acquired with this set-up from a 0.5-mm-thick cadmium sample (left) a 0.9-μm-thick tantalum sample (right). Spectra were acquired for about 10 min each when a current of about 180 μA was flowing in the ISIS synchrotron. The signal from the several capture resonances in cadmium and tantalum are quite evident as vertical lines. It is interesting to note how the T-PGAA spectra can be acquired down to TOF values of a fraction of μs with the fast YAP scintillators, corresponding to values of the neutron energy up to the MeV. As mentioned, as opposed to the case of cold and thermal neutron facilities, it is not possible at epithermal spectrometers to use curved guides to get rid of the γ-ray flash within the source and moderator. For this reason, at pulsed sources such as ISIS, the count rate during the first tens-to-hundreds of μs of the TOF measurement is extremely high. This is quite evident when looking at Fig. 4, where the

number of counts greatly increases for high neutron energies and low γ-ray energies.

Unfortunately, such high count rate is such that a standard HPGe detector is likely to saturate at short TOF values, then requiring ca. 50–100 μs of dead time before being operational again (see, e.g., Ref. [92]). This saturation of the detector allowed measurements up to ca. 5 eV in the case of VESUVIO ($L_0 \simeq 11$ m; TOF $\simeq 340$ μs) and ca. 60 eV in the case of INES ($L_0 \simeq 22$ m; TOF $\simeq 200$ μs). A similar situation is expected at ANNRI at J-PARC, where the sample position is at $L_0 \simeq 21.5$ m and NRCA measurements with Ge detectors were reported up to 300 eV [40]. Clearly, a shorter path length corresponds to an increase of the intensity of both neutron flux and background in the blockhouse, as well as reducing the peak resolution in NRCA spectra. However, increasing the value of L_0 one observes a quick decrease of the epithermal flux as, without an efficient guide, it is proportional to L_0^{-2}. This decrease is likely to affect, more than the T-PGAA technique, the DINS count rate. However, as already shown in Fig. 4, no saturation is expected for faster detectors such as the YAP scintillator used in this work. Fig. 5 shows the T-PGAA spectra using the HPGe detector on INES (left, reproduced from Ref. [104]) and the spectra from the same sample acquired on VESUVIO using the YAP scintillator described above. The capability to avoid saturation at low TOF values of the YAP has, as a counterpart, the inability to discriminate the many peaks from the gold γ-ray lines, as opposed to the measurement using the HPGe. It is also interesting to note that, though not completely saturating, the NRCA signal from the HPGe detector appears quite asymmetric, as if the signal following an intense resonance is spoiled by a partial saturation of the detector. This is quite evident in the case of the 4.9 eV neutron resonance of gold, appearing at ca. 360 μs on VESUVIO and 720 μs on INES.

3.3. Future developments

As previously mentioned, while the PGAA instrument blockhouses at reactor sources are bespoken so as to provide a low background, this is generally not the case at spallation neutron sources. The main reason, especially in the case of the VESUVIO and INES beamlines at ISIS, is related to the attempt to apply several techniques concurrently during the in-beam investigation of a given sample. The straightforward consequence of this attempt is that the sample is closely surrounded by several pieces of sample environment and detector banks, each with their shielding and electronics (see, e.g., Ref. [47]).

In this scenario, at present a tailored shielding is being manufactured at ISIS to be used on the HPGe detector available at the VESUVIO instrument [92]. The shielding is composed of an external layer of 5-cm-thick borated polyethylene (outer layer), followed by a 5-cm-thick pure lead, then a 1-mm-thick copper layer and, finally, a 1-mm-thick aluminium layer (inner layer). This design, pictorially shown in Fig. 6, is aimed at suppressing several sources of environmental background present at the instrument by shielding the HPGe detector against the direct radiation from the beam stop, the moderator, and the gold foils used for the resonance detector technique above-mentioned. In
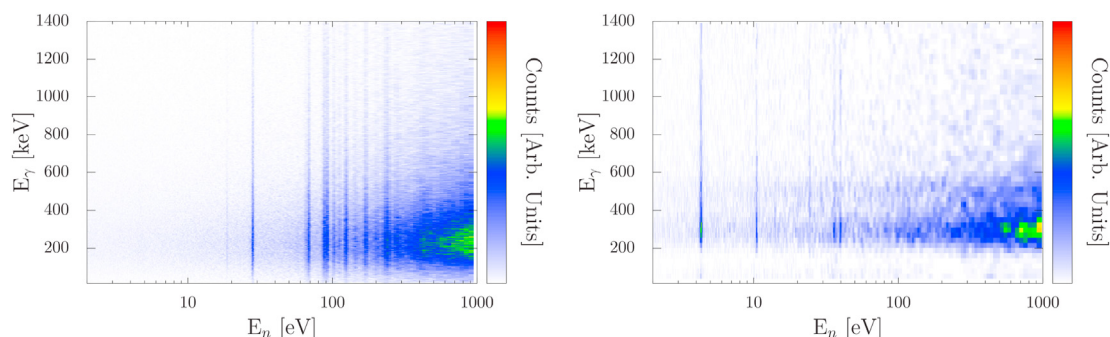

Fig. 4. T-PGAA spectra from cadmium (left) and tantalum (right) obtained at the VESUVIO spectrometer using a YAP detector.
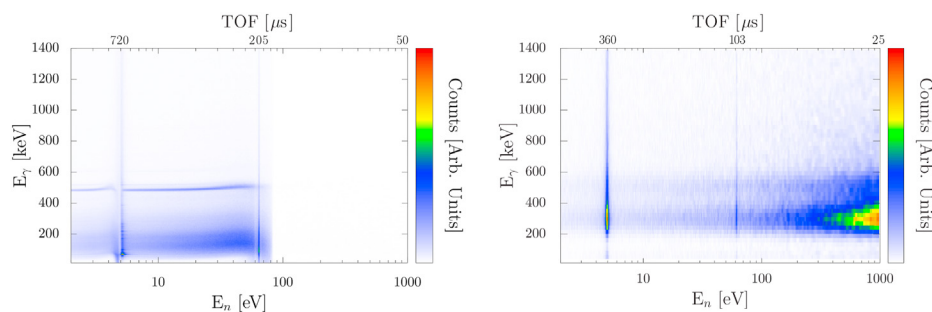
Fig. 5. T-PGAA spectra from Au obtained at the INES beamline using a HPGe detector (left), and at the VESUVIO spectrometer using a YAP detector (right).
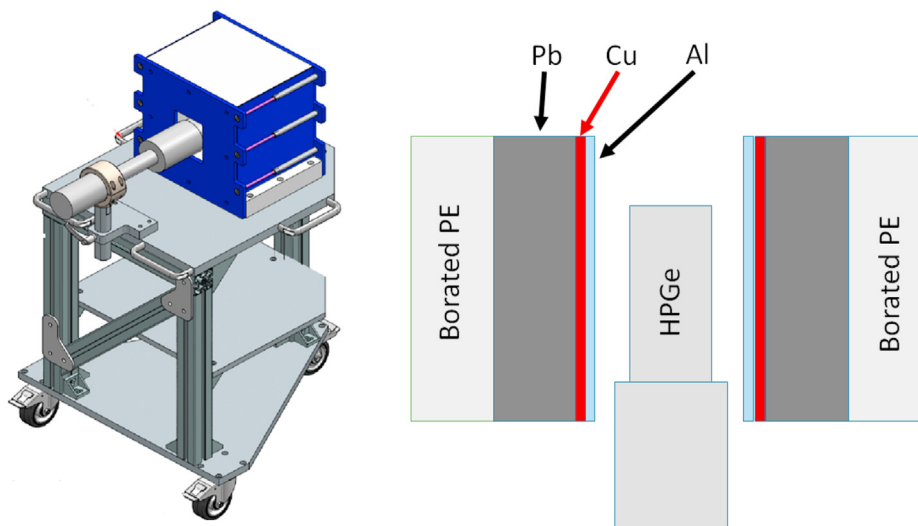

Fig. 6. A schematic drawing of the PGAA shielding being assembled at the VESUVIO spectrometer.

particular, given the mixed thermal/epithermal and γ-ray background in the blockhouse, the several layers have the following scope: 1) the external borated polyethylene is needed to slow-down and capture epithermal neutrons; 2) the pure lead is needed to shield against the γ-rays at 478 keV generated in the boron capture, as well as the several γ-rays from the gold foils, especially at energies between 200 and 300 keV bib102 [41,102], and other environmental radiation; and 3) the copper layer is needed to shield against the X-rays generated in the lead shielding, and the aluminium layer to stop the analogous X-rays from copper.

While, at dedicated beamlines, the shielding walls around the PGAA detector are generally thicker, this was not possible in the case of the VESUVIO instrument. In fact, the detector-plus-shielding system described above was designed so as to be mounted on a movable trolley. In this way, in the case of experiments where the T-PGAA capabilities are needed, or in the case of low-emitting samples, the detector can be moved closer to the sample position. However, as the additional shielding material around the HPGe detector is likely to cause additional background for the other detectors on the instrument, whenever the T-PGAA technique is not needed, the trolley can be moved further away from the sample position. It is also worth noting that, while this is not possible for the existing INES and VESUVIO instruments, future ETNA-like instruments can be designed so as to have larger blockhouses: this will decrease the environmental backgrounds from beam-stop and walls; it will allow several pieces of equipment, such as the PGAA trolley, to be moved freely towards and away from the sample area; and they will facilitate the handling of cultural-heritage samples that, in general, can be relatively large and bulky.

A possible way to have, at the same time, a higher epithermal flux and a long primary flight path, requires a suitable neutron source. In the case of ISIS, proton pulses generated in the synchrotron with a repetition rate of 50 Hz allow TOF measurements every 20 ms. One should notice that, both at the INES and VESUVIO beamlines, epithermal neutrons only populate the first ca. 1 ms of this period, while the rest is populated by thermal neutrons used for neutron diffraction. Therefore, in a future spallation neutron source, one can envisage a synchrotron working at a higher frequency, and three Target Stations (TSs), each with instruments dedicated to either cold (CTS), thermal (TTS), or epithermal (ETS) neutron techniques. Fig. 7 shows an example of how such source could work. The case suggested is clearly inspired by the current operations of the ISIS facility, where the TOF measurements in the TS1 and TS2 are 20-ms (40 Hz) and 100-ms long (10 Hz), respectively, and the epithermal instruments (such as VESUVIO and INES) are located in TS1. In particular, TS2 receives 1 proton pulse every 4 pulses directed to TS1. One can bring this model one step forward, and imagine a third TS where the frequency is further multiplied by a factor 4–5, or higher if possible, thus making the TOF acquisition periods shorter. In this way, epithermal neutrons could take advantage of a tailored repetition rate and TOF range. In order to avoid frame-overlap backgrounds, *i.e.*, to have slower neutrons being recorded at the same TOF value as faster neutrons from the following proton pulse, thermal filters, such as thick cadmium foils, could be inserted between the ETS moderator and the sample position of each of the epithermal instruments. Alternatively, neutron guides could be used to redirect the thermal component of the beam to another instrument, thus separating it from epithermal neutrons that would not be affected by the guide optics. While such high repetition rate represents a challenging project, compared to the more standard sources with 50-Hz repetition rates, it is interesting to notice how, already 20 years ago, a high repetition rate proton synchrotron was investigated by a JAERI-KEK
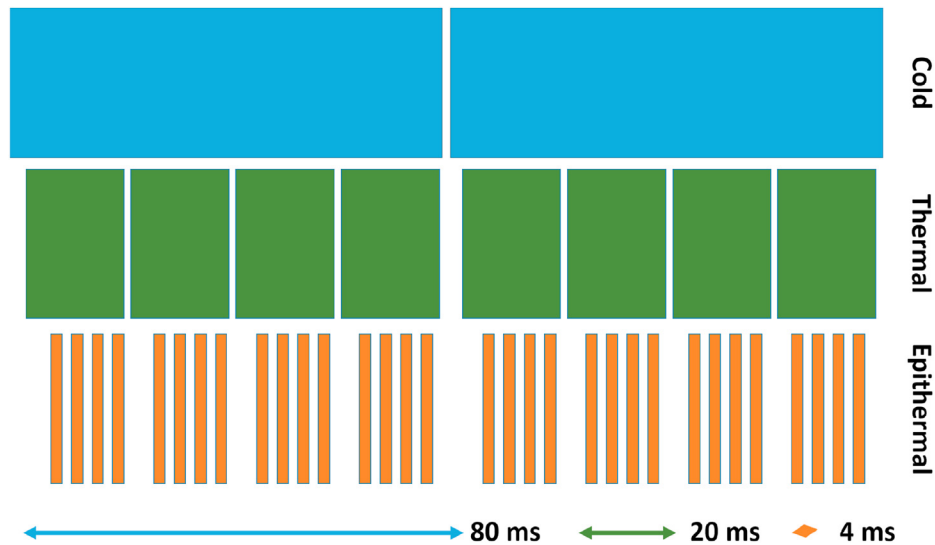
Fig. 7. The representation of possible TOF ranges at an imaginary 3-target-station spallation source with a proton synchrotron working at $f = 250$ Hz (5 times the ISIS frequency).

collaboration [105] to be used as a muon source. In this sense, a possible ETS could serve muon instruments as well. Moreover, high repetition rates are nowadays achieved at neutron sources based on electron linear accelerators (see, *e.g.,* Ref. [52] for a recent review).

4. Applications

4.1. Applications to cultural heritage

Several successful T-PGAA experiments and investigations have been possible over the past years (for further details on the experimental data, se Refs. [28,29,92]). Here, we would like to provide some synthetic examples of the most-likely applications of T-PGAA experiments on cultural-heritage artefacts.

In Fig. 2 we introduced the capture cross sections of copper and tin, the two main components of bronze, as well as the one for chlorine, an element that was found, using traditional PGAA, in Ref. [15] in the bronze panels of the Baptistery of Florence. Chloride components are responsible for the deterioration of bronze artefacts and, if present underneath gilded surface, they are relatively difficult to be detected using traditional surface probes. Also, from Fig. 1, it is evident that enhanced capabilities and detection limits compared to traditional PGAA would be of great importance for similar samples. Fig. 8 shows the macroscopic capture cross sections of the same elements from Fig. 2, and with a special focus in the region of epithermal neutron resonances. One can appreciate how, for slightly different values of the incident neutron energy, the capture cross section of each of the three elements can be orders of magnitude larger than the other two. From the inspection of this figure, one can clearly envisage the potentiality of the T-PGAA technique so as to enhance the signal from chlorine and allow a more accurate quantitative determination. Moreover, at an ETNA-like instrument, the T-PGAA results could be concurrently supported by neutron diffraction, to detect possible effects of the chlorides on the crystalline structure, or with neutron resonance transmission analysis [27] and energy-selective neutron imaging, so as to obtain a detailed 2D map of the chlorine distribution in the sample.

Based on the cross-section values reported in Figs. 2 and 8, one can estimate the count rate in a T-PGAA experiment based on the following equation

$$C(\Delta E_n, E_\gamma) = \Phi(E_n) \Delta E_n A \, d \, \rho \eta(E_\gamma) \Delta\Omega\Delta t \left(\sum_i \frac{\sigma_i(E_n, E_\gamma) w_i}{m_i m_N} \right), \quad (4)$$
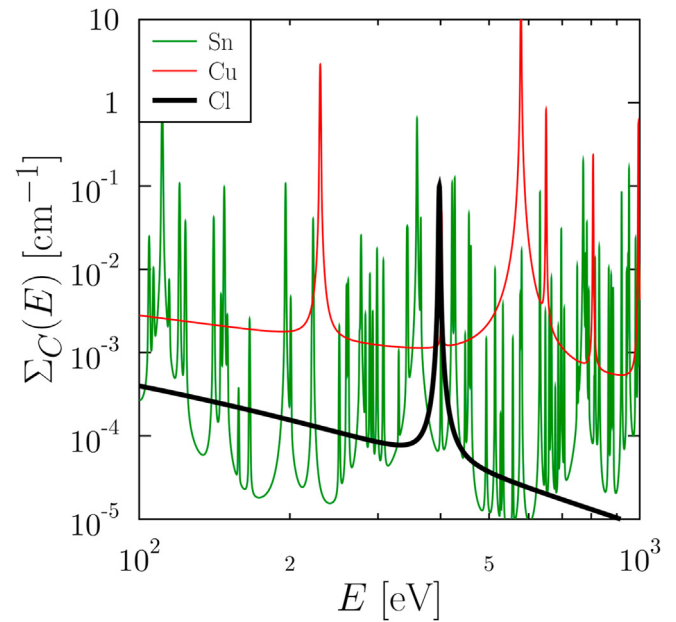

Fig. 8. Macroscopic cross section of bronze considering 88 %wt of natural copper, 0.12 %wt of natural tin, and 1 %wt of ^{137}Cl.

where A is the sample area perpendicular to the neutron beam, ρ its density and d its thickness; $C(\Delta E_n, E_\gamma)$ is the number of counts in a detector covering a solid angle $\Delta\Omega$ with respect to the sample position, after an acquisition time Δt for a γ-ray energy E_γ and having selected the neutron energy range $E_n \pm \Delta E_n/2$. Moreover, $\eta(E_\gamma)$ is the energy-dependent efficiency of the PGAA detector, $\sigma_i(E_n, E_\gamma)$ the microscopic capture cross section, multiplied by the emission probability of a γ-ray with energy E_γ, of the isotope i in the sample, with nuclear mass is m_i and weight percentage w_i. Finally, $\Phi(E_n)$ is the neutron flux at the sample position. Taking into considerations typical values in the case of the VESUVIO spectrometer, and the sample composition from Fig. 8, one obtains the parameters reported in Table 3.

Using the parameters from Table 3 and Equation (4), one can obtain the synthetic spectra in Fig. 9, in the special case of a HPGe and LaBr$_3$ detectors. The macroscopic capture cross section in Table 3 is

Table 3

Average values of the macroscopic capture cross section, $\Sigma_{n,\gamma}(\Delta E_n)$ for natural chlorine, copper, and tin, for several neutron energy ranges, ΔE_n, corresponding to the thermal energy region (0.003–0.04 eV), to the first neutron resonance in tin isotopes (38.6–39.0 eV), and the first neutron resonance in chlorine isotopes (396–399 eV). The value of the integrated VESUVIO flux over the same energy ranges, $\Phi(\Delta E_n)\Delta E_n$, is also reported.

ΔE_n [eV]	^{nat}Cl	$\Sigma_{n,\gamma}(\Delta E_n)$ [cm^{-1}] ^{nat}Cu	^{nat}Sn	$\Phi(\Delta E_n)\Delta E_n$ [n/cm^2/s]
0.003–0.04	0.077	**0.320**	0.0004	8.5×10^4
38.6–39.0	0.001	0.006	**0.025**	8.2×10^3
396–399	**0.075**	0.001	0.00001	7.3×10^3

proportional to the probability of capturing a neutron of a given energy and emitting a γ-ray of any energy, and it was multiplied by the probabilities to emit a particular γ-ray line in order to obtain the spectra in Fig. 9. For the sake of clarity, we have avoided to include any experimental backgrounds, for this topic has already been addressed elsewhere [28,29,92]. The first thing to notice is that, within an order of magnitude, the expected count rates from thermal and epithermal neutrons are comparable. This is an indication of the substantial amount of epithermal neutrons available, here in the specific case of the VESUVIO spectrometer, even in a narrow energy range within the full width at half maximum of a given resonance. Secondly, one can appreciate how the thermal-neutron spectrum, presenting many prompt-γ-ray peaks, can be largely simplified in the case of a T-PGAA measurement centred at a given neutron resonance. Moreover, as a lower number of peaks are present in the spectrum, one can relax the usual PGAA requirement of having a high-resolution (yet slow) detector, like a HPGe, and use a fast scintillating detector instead. In particular, as one can appreciate from Fig. 9, the two γ-ray lines from chlorine are likely to be easily analysable even with the lower resolution of the LaBr$_3$ scintillator, for the γ-ray lines from copper and tin at similar energies are completely negligible. Finally, the use of a fast scintillator, as opposed to a HPGe standard PGAA detector, is likely to allow T-PGAA measurements to energies much higher than those achieved in Refs. [28,29,92], possibly up to the MeV-neutron energies, available at the VESUVIO spectrometer within the first 5 μs in a TOF measurement.

4.2. Applications to security

The qualitative separation between the prompt γ-ray signal from fast and thermal neutrons, generally referred to Pulsed Fast and Thermal Neutron Activation (PFTNA), has found in recent decades several

applications in security and industrial topics bib106[23,106,107], such as the detection of explosives and narcotics. The technique is based on compact pulsed neutron sources of fast neutrons. A short pulse, of the order of 100 μs, is followed by a longer pause, of the order of 900 μs. The idea is to detect, during the short pulse, the prompt γ-rays resulting from the interaction of the fast neutrons, especially the nuclear inelastic interactions, then, during the longer pause, the signal from the prompt γ-rays following the capture of the lower-energy neutrons that were moderated and thermalized by the sample. The technique is particularly sensitive to the high-energy photons from the (n, n'γ) reactions in carbon (4439 keV), nitrogen (5106 keV) and oxygen (6130 keV), and makes use of the specific average ratios of carbon-to-nitrogen and carbon-to-oxygen content in explosives and narcotics, markedly different than from other organic materials.

In this framework, PFTNA apparatuses could be tested at T-PGAA instruments to further optimise their design and detection limits. In fact, one could take advantage of the neutron transmission technique at ETNA-like instruments for the measurement of the total cross section of a given sample, then of its moderation capabilities (see, e.g., Refs. [108,109]). Moreover, the punctual measurement of the PGAA signal for each TOF value, ideally up to the MeV neutron energies, would allow a more detailed characterization of the apparatus response, so as to go beyond the instrumental separation between fast and thermal neutrons based on a short irradiation pulse and a long thermalization pause.

4.3. Applications to radiation protection

Recently, a multi-technique investigation of the radiation-protection capabilities of barite-enriched concrete for radiation protection shielding was performed at VESUVIO [110]. Barium-containing compounds are generally included in concrete to increase the capture cross section for fast neutrons as well as to attenuate γ-rays [111]. The resulting shielding material is particularly suitable for applications at medical and research facilities with mixed neutron/γ-ray backgrounds. However, as the capture of fast neutrons by barium is accompanied by the emission of secondary γ-rays, the radiation-shielding capabilities of barite-enriched concrete need to be finely tuned over the amount of barium and the overall concrete geometry [112]. In the investigation above-mentioned [110], a number of pieces of information were collected at the same time, including the amount of hydrogen (as a neutron moderating agent) using deep-inelastic neutron scattering; the amount of barium using NRCA; the total macroscopic cross section using energy-resolved neutron transmission; and the atomic-scale structure using neutron diffraction.

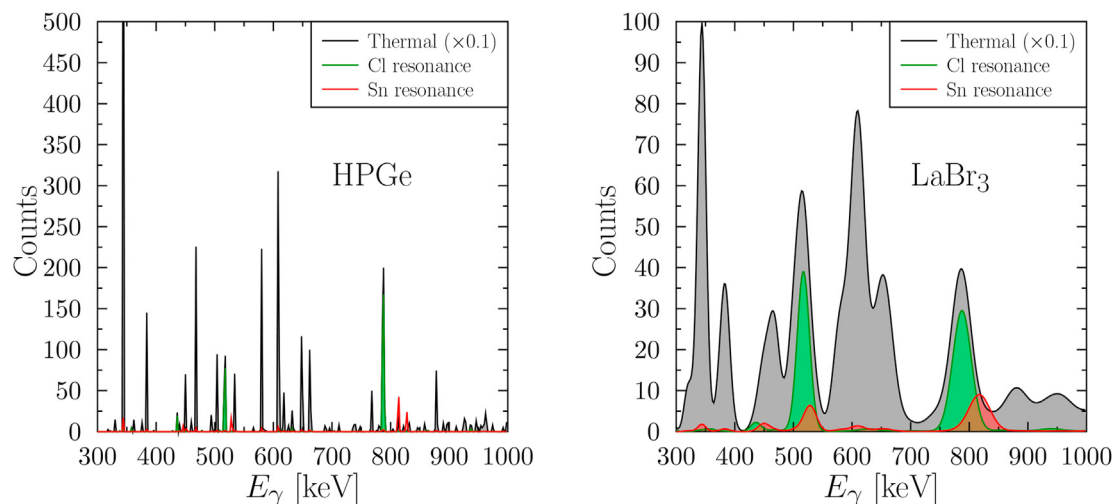However, one can imagine what an important piece of information

Fig. 9. Calculated T-PGAA spectra from a chlorine-containing bronze sample for the different neutron energy ranges introduced in Table 3. The calculated spectra are presented in the case of a HPGe (left) and detector and a LaBr$_3$ detector (right).

would be, in future investigations, the T-PGAA signal from the secondary γ-rays produced in the concrete sample. By making use of a trolley-like apparatus, as the one described above, one could investigate the intensities of prompt γ-rays as a function of the distance from the sample as well as the self-attenuation contribution of the shielding material to its own-generated γ-rays. One should note that, especially for fast neutrons, Monte Carlo investigations often rely on unresolved neutron capture cross section libraries, *i.e.*, libraries where the neutron capture cross section is not known in detail as a function of the incident neutron energy. Therefore, the use of a fast detector, such as a LaBr$_3$ scintillator, could allow measurements with a higher level of detail than the available predictions from Monte Carlo simulations. Moreover, as the required self-attenuation capabilities are dependent upon the sample geometry, a detailed experimental characterization using T-PGAA would be quite useful to benchmark computer simulations.

5. Outlook

Nowadays neutron-activation techniques, and especially traditional PGAA, are routinely used in two different scenarios. On the one side at reactor sources, where thermal and cold neutron energies are mainly employed. On the other side, at compact or portable neutron sources, where fast neutrons are employed and, for pulsed sources, they are discriminated against the signal from thermalized neutrons within the sample and surroundings. However, a gap has not been filled yet, that is the broad energy range between thermal and fast neutrons, *i.e.,* epithermal neutron energies from hundreds of meV to hundreds of keV, available using the TOF technique at spallation neutron sources.

The first steps to fill this gap have been walked over the last decade, so as to develop T-PGAA as a self-standing technique, especially at J-PARC and ISIS spallation neutron sources. However, based on the discussion presented here, additional capabilities, lower backgrounds, and optimized set-ups can be achieved. The development we suggest is twofold: on the one side, by decreasing the environmental background, more difficult to control at spallation sources with respect to reactor sources. On the other side, by accompanying standard HPGe detector, nowadays used for thermal and cold neutrons, with faster scintillators, such as LaBr$_3$ detectors. In the latter case, T-PGAA experiments will be available whereby the signal-to-background ratio to detect a given element is maximised by detecting the prompt γ-rays emitted after a resonantly captured neutron.

However, a new strategy in the γ-ray detection needs to be accompanied by a suitable design of the instrument blockhouse and of the facility in general. In particular, future spallation neutron sources interested to include T-PGAA capabilities in their scientific programmes, should consider a dedicated high-frequency under-moderated neutron target where beamlines using epithermal neutrons, as well as other techniques such as muon spectroscopy, could take advantage of a higher flux. This could be of interest both for ongoing projects, such as the European Spallation Source (at present under construction), as well as for future facilities, *e.g.,* in the framework of a future ISIS-II. Moreover, we have discussed how the technique could be employed on general-purpose instruments for materials characterization, as it is the case at present on the VESUVIO spectrometer at ISIS.

Our discussion shows that T-PGAA capabilities could support a number of scientific user programmes, from investigations of cultural-heritage artefacts, to materials for radiation-protections applications, including the test of security protocols and apparatuses for the detection of explosives. The continued interest in the technique and its development in the last years, both at ISIS and J-PARC, are the best proof that T-PGAA at spallation neutron sources will significantly contribute to neutron-based investigations over the next decades.

CRediT authorship contribution statement

Giovanni Romanelli: Investigation, Methodology, Writing – original

draft. **Giulia Festa:** Investigation, Methodology, Writing – review & editing. **Dalila Onorati:** Investigation. **Enrico Preziosi:** Writing – original draft. **Pierfrancesco Ulpiani:** Investigation. **Carla Andreani:** Writing – review & editing. **Roberto Senesi:** Conceptualization, Writing – review & editing.

Declaration of competing interest

The authors declare that they have no known competing financial interests or personal relationships that could have appeared to influence the work reported in this paper.

Acknowledgements

References

[1] G.E. Boyd, Method of activation analysis, Anal. Chem. 21 (3) (1949) 335–347, https://doi.org/10.1021/ac60027a005.

[2] T.I. Taylor, R.H. Anderson, W.W. Havens, Chemical analysis by neutron spectroscopy, Science 114 (2962) (1951) 341–355, https://doi.org/10.1126/science.114.2962.341.

[3] G. v. Hevesy, H. Levi, Artificial activity of hafnium and some other elements, Kgl. Danske Videnskab. Selskab: Math-Fys. Medd. 15 (11).

[4] G.T. Seaborg, J.J. Livingood, Artificial radioactivity as a test for minute traces of elements, J. Am. Chem. Soc. 60 (8) (1938) 1784–1786, https://doi.org/10.1021/ja01275a018.

[5] V. Guinn, C. Wagner, Instrumental neutron activation analysis, Anal. Chem. 32 (3) (1960) 317–323.

[6] W.H. Zoller, G.E. Gordon, Instrumental neutron activation analysis of atmospheric pollutants utilizing ge (li) gamma-ray detectors, Anal. Chem. 42 (2) (1970) 257–265.

[7] J.M. Ondov, W. Zoller, I. Olmez, N. Aras, G. Gordon, L. Rancitelli, K. Abel, R.H. Filby, K. Shah, R. Ragaini, Elemental concentrations in the national bureau of standards' environmental coal and fly ash standard reference materials, Anal. Chem. 47 (7) (1975) 1102–1109.

[8] M.P. Failey, D.L. Anderson, W.H. Zoller, G.E. Gordon, R.M. Lindstrom, Neutron-capture prompt. gamma.-ray activation analysis for multielement determination in complex samples, Anal. Chem. 51 (13) (1979) 2209–2221.

[9] A.H. Beddoe, H. Zudmeer, G.L. Hill, A prompt gamma in vivo neutron activation analysis facility for measurement of total body nitrogen in the critically ill, Phys. Med. Biol. 29 (4) (1984) 371–383, https://doi.org/10.1088/0031-9155/29/4/007.

[10] E.V. Sayre, R.W. Dodson, D.B. Thompson, Neutron activation study of mediterranean potsherds, Am. J. Archaeol. 61 (1) (1957) 35–41.

[11] V.M. Emeleus, G. Simpson, Neutron activation analysis of ancient roman potsherds, Nature 185 (4707) (1960), 196–196.

[12] Nuclear Techniques for Cultural Heritage Research, No. 2 in Radiation Technology Series, INTERNATIONAL ATOMIC ENERGY AGENCY, Vienna, 2011.

[13] G. Gorini, The Ancient Charm Collaboration, Ancient Charm: a research project for neutron-based investigation of cultural-heritage objects, Nuovo Cimento C Geophysics Space Physics C 30 (2007) 47–58, https://doi.org/10.1393/ncc/i2006-10035-9.

[14] T. Belgya, Z. Kis, L. Szentmiklósi, Z. Kasztovszky, P. Kudejova, R. Schulze, T. Materna, G. Festa, P. Caroppi, First elemental imaging experiments on a combined PGAI and NT setup at the budapest research reactor, J. Radioanal. Nucl. Chem. 278 (3) (2008) 751–754.

[15] G. Festa, C. Andreani, M.P. De Pascale, R. Senesi, G. Vitali, S. Porcinai, A.M. Giusti, R. Schulze, L. Canella, P. Kudejova, M. Mühlbauer, B. Schillinger, A nondestructive stratigraphic and radiographic neutron study of lorenzo ghiberti's reliefs from paradise and north doors of florence baptistery, J. Appl. Phys. 106 (7) (2009), 074909, https://doi.org/10.1063/1.3204514.

[16] C. Andreani, F. Aliotta, L. Arcidiacono, M. Borla, D. Di Martino, F. Facchetti, E. Ferraris, G. Festa, G. Gorini, W. Kockelmann, J. Kelleher, D. Malfitana, D. Micieli, T. Minniti, E.P. Cippo, R. Ponterio, G. Salvato, R. Senesi, V. Turina, C. Vasi, C. Greco, A neutron study of sealed pottery from the grave-goods of kha

and merit, J. Anal. At. Spectrom. 32 (2017) 1342–1347, https://doi.org/10.1039/C7JA00099E.

[17] G. Festa, T. Christiansen, V. Turina, M. Borla, J. Kelleher, L. Arcidiacono, L. Cartechini, R. Ponterio, C. Scatigno, R. Senesi, et al., Egyptian metallic inks on textiles from the 15 th century bce unravelled by non-invasive techniques and chemometric analysis, Sci. Rep. 9 (1) (2019) 1–8.

[18] G. Festa, T. Minniti, L. Arcidiacono, M. Borla, D. Di Martino, F. Facchetti, E. Ferraris, V. Turina, W. Kockelmann, J. Kelleher, et al., Egyptian grave goods of kha and merit studied by neutron and gamma techniques, Angew. Chem. 130 (25) (2018) 7497–7501.

[19] Z. Kasztovszky, K.T. Biró, A. Markó, V. Dobosi, Cold neutron prompt gamma activation analysis—a non-destructive method for characterization of high silica content chipped stone tools and raw materials, Archaeometry 50 (1) (2008) 12–29, https://doi.org/10.1111/j.1475-4754.2007.00348.x.

[20] R. Paul, R. Lindstrom, Prompt gamma-ray activation analysis: fundamentals and applications, J. Radioanal. Nucl. Chem. 243 (1) (2000) 181–189.

[21] G. Festa, G. Romanelli, R. Senesi, L. Arcidiacono, C. Scatigno, S. F. Parker, M. P. M. Marques, C. Andreani, Neutrons for cultural heritage—techniques, sensors, and detection, Sensors 20 (2). doi:10.3390/s20020502..

[22] R.M. Lindstrom, Z. Révay, Prompt gamma neutron activation analysis (PGAA): recent developments and applications, J. Radioanal. Nucl. Chem. 314 (2) (2017) 843–858.

[23] M. Litz, C. Waits, J. Mullins, Neutron-activated gamma-emission: Technology review; arl-tr-5871, Tech. Rep (2012). URL, https://apps.dtic.mil/sti/citations/ADA554870.

[24] R.M. Lindstrom, Prompt-gamma activation analysis, J. Res. Nat. Ins. Standards Technol. 98 (1) (1993) 127.

[25] G. Molnar, Handbook of Prompt Gamma Activation Analysis: with Neutron Beams, vol. 1, Springer Science & Business Media, 2004.

[26] D. Brown, M. Chadwick, R. Capote, A. Kahler, A. Trkov, M. Herman, A. Sonzogni, Y. Danon, A. Carlson, others, Endf/b-viii.0: the 8th major release of the nuclear reaction data library with cielo-project cross sections, new standards and thermal scattering data, Nucl. Data Sheets 148 (2018) 1–142, https://doi.org/10.1016/j.nds.2018.02.001, special Issue on Nuclear Reaction Data.

[27] H. Postma, P. Schillebeeckx, Neutron Resonance Capture and Transmission Analysis, John Wiley & Sons, Ltd, 2006, https://doi.org/10.1002/9780470027318.a9070.

[28] Y. Toh, M. Ebihara, A. Kimura, S. Nakamura, H. Harada, K.Y. Hara, M. Koizumi, F. Kitatani, K. Furutaka, Synergistic effect of combining two nondestructive analytical methods for multielemental analysis, Anal. Chem. 86 (24) (2014) 12030–12036, https://doi.org/10.1021/ac502632w.

[29] G. Festa, L. Arcidiacono, A. Pappalardo, T. Minniti, C. Cazzaniga, A. Scherillo, C. Andreani, R. Senesi, Isotope identification capabilities using time resolved prompt gamma emission from epithermal neutrons, J. Instrum. 11 (3) (2016), https://doi.org/10.1088/1748-0221/11/03/c03060. C03060–C03060.

[30] G.J. Atchison, W.H. Beamer, Neutron activation analysis with van de graaff accelerator, Anal. Chem. 28 (2) (1956) 237–243.

[31] W. Murphy, New service to analysts, Anal. Chem. 24 (8) (1952), https://doi.org/10.1021/ac60068a600, 1235–1235.

[32] W.W. Meinke, R.E. Anderson, Activation analysis using low level neutron sources, Anal. Chem. 25 (5) (1953) 778–783.

[33] M. Rossbach, Multielement prompt .gamma. cold neutron activation analysis of organic matter, Anal. Chem. 63 (19) (1991) 2156–2162, https://doi.org/10.1021/ac00019a016.

[34] C. Yonezawa, Prompt γ-ray analysis of elements using cold and thermal reactor guided neutron beams, Anal. Sci. 9 (2) (1993) 185–193.

[35] G. Molnár, T. Belgya, L. Dabolczi, B. Fazekas, Z. Révay, Á. Veres, I. Bikit, Z. Kiss, J. Östör, The new prompt gamma-activation analysis facility at budapest, J. Radioanal. Nucl. Chem. 215 (1) (1997) 111–115.

[36] L. Canella, P. Kudějová, R. Schulze, A. Türler, J. Jolie, Characterisation and optimisation of the new prompt gamma-ray activation analysis (PGAA) facility at frm ii, Nucl. Instrum. Methods Phys. Res. Sect. A Accel. Spectrom. Detect. Assoc. Equip. 636 (1) (2011) 108–113, https://doi.org/10.1016/j.nima.2011.01.126.

[37] M. Crittin, J. Kern, J.-L. Schenker, The new prompt gamma-ray activation facility at the Paul scherrer institute, Switzerland, Nucl. Instrum. Methods Phys. Res. Sect. A Accel. Spectrom. Detect. Assoc. Equip. 449 (1) (2000) 221–236, https://doi.org/10.1016/S0168-9002(99)01467-9.

[38] M. Frontasyeva, S. Pavlov, Analytical investigations at the ibr-2 reactor in dubna, Tech. rep (2000).

[39] J. Granada, R. Mayer, J. Dawidowski, J. Santisteban, F. Cantargi, J. Blostein, L.R. Palomino, A. Tartaglione, The sciences and applications of the electron linac-driven neutron source in Argentina, The European Physical Journal Plus 131 (6) (2016) 1–12.

[40] A. Kimura, T. Fujii, S. Fukutani, K. Furutaka, S. Goko, K.Y. Hara, H. Harada, K. Hirose, J. ichi Hori, M. Igashira, T. Kamiyama, T. Katabuchi, T. Kin, K. Kino, F. Kitatani, Y. Kiyanagi, M. Koizumi, M. Mizumoto, S. Nakamura, M. Ohta, M. Oshima, K. Takamiya, Y. Toh, Neutron-capture cross-sections of 244cm and 246cm measured with an array of large germanium detectors in the annri at j-parc/mlf, J. Nucl. Sci. Technol. 49 (7) (2012) 708–724, https://doi.org/10.1080/00223131.2012.693887.

[41] D. Onorati, G. Romanelli, P. Ulpiani, C. Cazzaniga, E. Preziosi, L. Arcidiacono, G. Festa, C. Andreani, R. Senesi, M.C. Morone, Fluka simulations and benchmark measurements of the yap(ce) scintillators installed on the vesuvio spectrometer, Nucl. Instrum. Methods Phys. Res. Sect. A Accel. Spectrom. Detect. Assoc. Equip. 969 (2020) 164012, https://doi.org/10.1016/j.nima.2020.164012.

[42] R.L. Paul, R.M. Lindstrom, A. Heald, Cold neutron prompt gamma-ray activation analysis at nist—recent developments, J. Radioanal. Nucl. Chem. 215 (1) (1997) 63–68.

[43] R.L. Paul, D. Şahin, J.C. Cook, C. Brocker, R.M. Lindstrom, D.J. O'Kelly, Ngd cold-neutron prompt gamma-ray activation analysis spectrometer at nist, J. Radioanal. Nucl. Chem. 304 (2) (2015) 189–193.

[44] Z. Révay, P. Kudějová, K. Kleszcz, S. Söllradl, C. Genreith, In-beam activation analysis facility at mlz, garching, Nucl. Instrum. Methods Phys. Res. Sect. A Accel. Spectrom. Detect. Assoc. Equip. 799 (2015) 114–123, https://doi.org/10.1016/j.nima.2015.07.063.

[45] F. Fernandez-Alonso, D.L. Price, Neutron Scattering – Fundamentals, Academic Press, New York, 2013.

[46] V.F. Sears, Neutron scattering lengths and cross sections, Neutron News 3 (3) (1992) 26–37, https://doi.org/10.1080/10448639208218770.

[47] G. Romanelli, M. Krzystyniak, R. Senesi, D. Raspino, J. Boxall, D. Pooley, S. Moorby, E. Schooneveld, N.J. Rhodes, C. Andreani, F. Fernandez-Alonso, Characterisation of the incident beam and current diffraction capabilities on the vesuvio spectrometer, Meas. Sci. Technol. 28 (9) (2017), 095501.

[48] R. Zeisler, G.P. Lamaze, H.H. Chen-Mayer, Coincidence and anti-coincidence measurements in prompt gamma neutron activation analysis with pulsed cold neutron beams, J. Radioanal. Nucl. Chem. 248 (1) (2001) 35–38.

[49] L. Szentmiklósi, T. Belgya, Z. Révay, Z. Kis, Upgrade of the prompt gamma activation analysis and the neutron-induced prompt gamma spectroscopy facilities at the budapest research reactor, J. Radioanal. Nucl. Chem. 286 (2) (2010) 501–505.

[50] R. Senesi, A.I. Kolesnikov, C. Andreani, Measurement of proton momentum distributions using a direct geometry instrument, J. Phys. Conf. Ser. 571 (1) (2014), 012007.

[51] T.R. Prisk, A.I. Kolesnikov, G.E. Granroth, J.-L. Lin, B.J. Heuser, Vibrational modes and quantum zero-point energy of hydrogen in zrh0.0155 and zrh2, J. Alloys Compd. 818 (2020) 152832, https://doi.org/10.1016/j.jallcom.2019.152832.

[52] I. Anderson, C. Andreani, J. Carpenter, G. Festa, G. Gorini, C.-K. Loong, R. Senesi, Research opportunities with compact accelerator-driven neutron sources, URL, Phys. Rep. 654 (2016) 1–58, https://doi.org/10.1016/j.physrep.2016.07.007. research opportunities with compact accelerator-driven neutron sources, https://www.sciencedirect.com/science/article/pii/S0370157316301958.

[53] J. prepared, Managed by the TUM, IAEA, Tech. rep, URL, https://nucleus.iaea.org/RRDB/Uploads/RR%20Applications/PGNAA%20Facilities%20Database%20v2015-02-19.pdf, 2015.

[54] T. Katabuchi, Y. Toh, M. Mizumoto, T. Saito, K. Terada, A. Kimura, S. Nakamura, H. Minghui, G. Rovira, M. Igashira, Discovery of a new low energy neutron resonance of ^{89}y, The European Physical Journal A 57 (1) (2021) 1–4.

[55] E.S. Gladney, E.T. Jurney, D.B. Curtis, Nondestructive determination of boron and cadmium in environmental materials by thermal neutron-prompt gamma-ray spectrometry, Anal. Chem. 48 (14) (1976) 2139–2142, https://doi.org/10.1021/ac50008a021.

[56] S.F. Parker, F. Fernandez-Alonso, A.J. Ramirez-Cuesta, J. Tomkinson, S. Rudic, R.S. Pinna, G. Gorini, J.F. Castañon, Recent and future developments on tosca at isis, J. Phys. Conf. Ser. 554 (1) (2014), 012003.

[57] A. Miceli, G. Festa, R. Senesi, E.P. Cippo, L. Giacomelli, M. Tardocchi, A. Scherillo, E. Schooneveld, C. Frost, G. Gorini, C. Andreani, Measurements of gamma-ray background spectra at spallation neutron source beamlines, Journal of Applied Analytical Spectroscopy 29 (2014) 1897–1903, https://doi.org/10.1039/C4JA00183D.

[58] G. Festa, C. Andreani, L. Arcidiacono, G. Burca, W. Kockelmann, T. Minniti, R. Senesi, Characterization of γ-ray background at IMAT beamline of ISIS spallation neutron source, J. Instrum. 12 (8) (2017), https://doi.org/10.1088/1748-0221/12/08/p08005. P08005–P08005.

[59] D. Onorati, C. Andreani, L. Arcidiacono, F. Fernandez-Alonso, G. Festa, M. Krzystyniak, G. Romanelli, P. Ulpiani, R. Senesi, Gamma background characterization on VESUVIO: before and after the moderator upgrade, J. Phys. Conf. Ser. 1055 (2018), 012009, https://doi.org/10.1088/1742-6596/1055/1/012009.

[60] Z. Kasztovszky, W. Kockelmann, E. Perelli Cippo, G. Gorini, M. Tardocchi, Prompt gamma activation studies on archaeological objects at a pulsed neutron source, Il Nuovo Cimento C 31 (2) (2008) 143–155.

[61] C. Yonezawa, A.K.H. Wood, M. Hoshi, Y. Ito, E. Tachikawa, The characteristics of the prompt gamma-ray analyzing system at the neutron beam guides of jrr-3m, Nucl. Instrum. Methods Phys. Res. Sect. A Accel. Spectrom. Detect. Assoc. Equip. 329 (1) (1993) 207–216, https://doi.org/10.1016/0168-9002(93)90938-E.

[62] M. Gierlik, S. Borsuk, Z. Guzik, J. Iwanowska, S. Korolczuk, T. Kozłowski, T. Krakowski, R. Marcinkowski, L. Swiderski, M. Szeptycka, et al., Application of the anti-compton detector in neutron activation analysis techniques, Nucl. Instrum. Methods Phys. Res. Sect. A Accel. Spectrom. Detect. Assoc. Equip. 788 (2015) 54–58.

[63] http://scintillator.lbl.gov/, Scintillation properties (Last accessed on February 2021)..

[64] G.F. Knoll, Radiation Detection and Measurement, John Wiley & Sons, 2010.

[65] R. Britton, Compton suppression systems for environmental radiological analysis, J. Radioanal. Nucl. Chem. 292 (1) (2012) 33–39.

[66] J. F. Briesmeister, et al., Mcnptm-a General Monte Carlo N-Particle Transport Code, Version 4C, LA-13709-M, Los Alamos National Laboratory vol. 2..

[67] L. Szentmiklósi, Z. Kis, T. Belgya, A.N. Berlizov, On the design and installation of a compton–suppressed hpge spectrometer at the budapest neutron-induced prompt gamma spectroscopy (nips) facility, J. Radioanal. Nucl. Chem. 298 (3) (2013) 1605–1611.

[68] S. Agostinelli, J. Allison, K.a. Amako, J. Apostolakis, H. Araujo, P. Arce, M. Asai, D. Axen, S. Banerjee, G. Barrand, et al., Geant4—a simulation toolkit, Nucl. Instrum. Methods Phys. Res. Sect. A Accel. Spectrom. Detect. Assoc. Equip. 506 (3) (2003) 250–303.

[69] N. Shun-Li, C. Xiao, W. Zhen-Zhong, L. Yi, X. Yu-Guang, Y. Bo-Xiang, W. Zhi-Gang, F. Jian, S. Xi-Lei, S. Li-Jun, et al., Simulation of background reduction and compton suppression in a low-background hpge spectrometer at a surface laboratory, Chin. Phys. C 39 (8) (2015), 086002.

[70] M. Fechner, C. Henson, J. Gaffiot, T. Lasserre, A. Letourneau, D. Lhuillier, G. Mention, T.A. Mueller, R. Quéval, R. Svoboda, A large hpge detector for the non-destructive radioassay of an ultra-low-background counting facility, Appl. Radiat. Isot. 69 (7) (2011) 1033–1038.

[71] A. Ferrari, J. Ranft, P.R. Sala, A. Fassò, FLUKA: A Multi-Particle Transport Code (Program Version 2005), No, CERN-2005-10, Cern, 2005.

[72] J.L. Orrell, C.E. Aalseth, J.F. Amsbaugh, P.J. Doe, T.W. Hossbach, Operation of a high-purity germanium crystal in liquid argon as a compton-suppressed radiation spectrometer, Nucl. Instrum. Methods Phys. Res. Sect. A Accel. Spectrom. Detect. Assoc. Equip. 579 (1) (2007) 91–93.

[73] C. Robert, G. Dedes, G. Battistoni, T. Böhlen, I. Buvat, F. Cerutti, M. Chin, A. Ferrari, P. Gueth, C. Kurz, et al., Distributions of secondary particles in proton and carbon-ion therapy: a comparison between gate/geant4 and fluka Monte Carlo codes, Phys. Med. Biol. 58 (9) (2013) 2879.

[74] J. Krimmer, D. Dauvergne, J. Létang, É. Testa, Prompt-gamma monitoring in hadrontherapy: a review, Nucl. Instrum. Methods Phys. Res. Sect. A Accel. Spectrom. Detect. Assoc. Equip. 878 (2018) 58–73.

[75] A.-C. Knopf, A. Lomax, In vivo proton range verification: a review, Phys. Med. Biol. 58 (15) (2013) R131.

[76] J. Cooper, R. Perkins, A versatile ge (li)-nai (tl) coincidence-anticoincidence gamma-ray spectrometer for environmental and biological problems, Nucl. Instrum. Methods 99 (1) (1972) 125–146.

[77] A. Wrońska, et al., Prompt gamma imaging in proton therapy-status, challenges and developments, in: Journal of Physics: Conference Series, vol. 1561, IOP Publishing, 2020, 012021.

[78] L. Kelleter, A. Wrońska, J. Besuglow, A. Konefał, K. Laihem, J. Leidner, A. Magiera, K. Parodi, K. Rusiecka, A. Stahl, et al., Spectroscopic study of prompt-gamma emission for range verification in proton therapy, Phys. Med. 34 (2017) 7–17.

[79] F. Hueso-González, F. Fiedler, C. Golnik, T. Kormoll, G. Pausch, J. Petzoldt, K.E. Römer, W. Enghardt, Compton camera and prompt gamma ray timing: two methods for in vivo range assessment in proton therapy, Frontiers in oncology 6 (2016) 80.

[80] Z. Yao, Y. Xiao, Z. Chen, B. Wang, Q. Hou, Compton-based prompt gamma imaging using ordered origin ensemble algorithm with resolution recovery in proton therapy, Sci. Rep. 9 (1) (2019) 1–15.

[81] J.M. Verburg, K. Riley, T. Bortfeld, J. Seco, Energy-and time-resolved detection of prompt gamma-rays for proton range verification, Phys. Med. Biol. 58 (20) (2013) L37.

[82] F. Hueso-González, M. Rabe, T.A. Ruggieri, T. Bortfeld, J.M. Verburg, A full-scale clinical prototype for proton range verification using prompt gamma-ray spectroscopy, Phys. Med. Biol. 63 (18) (2018) 185019.

[83] J. Polf, S. Peterson, M. McCleskey, B. Roeder, A. Spiridon, S. Beddar, L. Trache, Measurement and calculation of characteristic prompt gamma ray spectra emitted during proton irradiation, Phys. Med. Biol. 54 (22) (2009) N519.

[84] J.M. Verburg, J. Seco, Proton range verification through prompt gamma-ray spectroscopy, Phys. Med. Biol. 59 (23) (2014) 7089.

[85] https://www.isis.stfc.ac.uk/Pages/ISIS II.aspx (Last accessed on January 2021)..

[86] A. Pietropaolo, R. Senesi, Electron Volt neutron spectrometers, Phys. Rep. 508 (2011) 45–90, https://doi.org/10.1016/j.physrep.2011.07.0`1.

[87] C. Andreani, A. Pietropaolo, R. Senesi, G. Gorini, M. Tardocchi, A. Bracco, N. Rhodes, E. Schooneveld, Electron-volt spectroscopy at a pulsed neutron source using a resonance detector technique, Nucl. Instrum. Methods A 481 (2002) 509–520, https://doi.org/10.1016/S0168-9002(01)01412-7.

[88] E.M. Schooneveld, J. Mayers, N.J. Rhodes, A. Pietropaolo, C. Andreani, R. Senesi, G. Gorini, E. Perelli-Cippo, M. Tardocchi, Foil cycling technique for the VESUVIO spectrometer operating in the resonance detector configuration, Rev. Sci. Instrum. 77 (2006) 5103, https://doi.org/10.1063/1.2349598.

[89] M. Tardocchi, G. Gorini, A. Pietropaolo, C. Andreani, R. Senesi, N. Rhodes, E.M. Schooneveld, YAP scintillators for resonant detection of epithermal neutrons at pulsed neutron sources, Rev. Sci. Instrum. 75 (2004) 4880–4890, https://doi.org/10.1063/1.1795091.

[90] C. Andreani, A. D'Angelo, G. Gorini, S. Imberti, A. Pietropaolo, N.J. Rhodes, E.M. Schooneveld, R. Senesi, M. Tardocchi, CdZnTe γ detector for deep inelastic neutron scattering on the VESUVIO spectrometer, Appl. Phys. Mater. Sci. Process 78 (2004) 903–913, https://doi.org/10.1007/s00339-003-2087-7.

[91] S. Imberti, W. Kockelmann, M. Celli, F. Grazzi, M. Zoppi, A. Botti, A. Sodo, M.L. Imperiale, M. de Vries-Melein, D. Visser, H. Postma, Neutron diffractometer INES for quantitative phase analysis of archaeological objects, Meas. Sci. Technol. 19 (3) (2008), 034003, https://doi.org/10.1088/0957-0233/19/3/034003.

[92] L. Arcidiacono, M. Martinón-Torres, R. Senesi, A. Scherillo, C. Andreani, G. Festa, Cu-based alloys as a benchmark for T-PGAA quantitative analysis at spallation neutron sources, J. Anal. At. Spectrom. 35 (2020) 331–340, https://doi.org/10.1039/C9JA00268E.

[93] M. Krzystyniak, G. Romanelli, M. Fabian, M. Gutmann, G. Festa, L. Arcidiacono, M. Gigg, K. Drużdot, C. Andreani bicki, R. Senesi, F. Fernandez-Alonso, Vesuvio+: the current testbed for a next-generation epithermal neutron spectrometer, J. Phys. Conf. Ser. 1021 (1) (2018), 012026.

[94] C. Andreani, D. Colognesi, J. Mayers, G.F. Reiter, R. Senesi, Measurement of momentum distribution of light atoms and molecules in condensed matter systems using inelastic neutron scattering, Adv. Phys. 54 (5) (2005) 377–469, https://doi.org/10.1080/00018730500403136.

[95] C. Andreani, M. Krzystyniak, G. Romanelli, R. Senesi, F. Fernandez-Alonso, Electron-volt neutron spectroscopy: beyond fundamental systems, Adv. Phys. 66 (1) (2017) 1–73, https://doi.org/10.1080/00018732.2017.1317963.

[96] G. Romanelli, M. Krzystyniak, G. Festa, C. Andreani, F. Fernandez-Alonso, R. Senesi, The road to a station for epithermal and thermal neutron analysis, J. Phys. Conf. Ser. 1055 (1) (2018), 012017.

[97] M. Krzystyniak, G. Romanelli, F. Fernandez-Alonso, Non-destructive quantitation of hydrogen via mass-resolved neutron spectroscopy, Analyst 144 (2019) 3936–3941, https://doi.org/10.1039/C8AN01729H.

[98] G. Romanelli, M. Krzystyniak, F. Fernandez-Alonso, Neutron-resonance capture analysis on the VESUVIO spectrometer: towards high-throughput material characterisation, J. Phys. Conf. 1055 (2018), 012015, https://doi.org/10.1088/1742-6596/1055/1/012015.

[99] J. Robledo, J. Dawidowski, J.M. Damián, G. Škoro, C. Bovo, G. Romanelli, Measurement of neutron total cross sections at the vesuvio spectrometer, Nucl. Instrum. Methods Phys. Res., Sect. A 969 (2020) 164096, https://doi.org/10.1016/j.nima.2020.164096.

[100] T. Kemper, S. Sommer, Estimate of heavy metal contamination in soils after a mining accident using reflectance spectroscopy, Environ. Sci. Technol. 36 (12) (2002) 2742–2747, https://doi.org/10.1021/es015747j.

[101] G. Maccauro, P.R. Iommetti, F. Muratori, L. Raffaelli, P.F. Manicone, C. Fabbriciani, An overview about biomedical applications of micron and nano size tantalum, Recent Pat. Biotechnol. 3 (3) (2009) 157–165.

[102] P. Ulpiani, G. Romanelli, D. Onorati, A. Parmentier, G. Festa, E. Schooneveld, C. Cazzaniga, L. Arcidiacono, C. Andreani, R. Senesi, Optimization of detection strategies for epithermal neutron spectroscopy using photon-sensitive detectors, Rev. Sci. Instrum. 90 (7) (2019), 073901, https://doi.org/10.1063/1.5091084.

[103] P. Ulpiani, G. Romanelli, D. Onorati, M. Krzystyniak, C. Andreani, R. Senesi, The effective isotropy of the hydrogen local potential in biphenyl and other hydrocarbons, J. Chem. Phys. 153 (23) (2020) 234306, https://doi.org/10.1063/5.0029578.

[104] P. Ulpiani, G. Romanelli, L. Arcidiacono, D. Onorati, G. Festa, M. Krzystyniak, E. Schooneveld, F. Fernandez-Alonso, C. Andreani, R. Senesi, Enhancement of counting statistics and noise reduction in the forward-scattering detectors on the vesuvio spectrometer, J. Phys. Conf. Ser. 1055 (1) (2018), 012008.

[105] Y. Ishi, Y. Mori, M. Muto, Y. Shirakabe, A. Takagi, High field, high repetition rate kicker, Nucl. Instrum. Methods Phys. Res. Sect. A Accel. Spectrom. Detect. Assoc. Equip. 472 (3) (2001) 639–642, https://doi.org/10.1016/S0168-9002(01)01323-7, nuFACT2000.

[106] G. Vourvopoulos, P. Womble, Pulsed fast/thermal neutron analysis: a technique for explosives detection, Talanta 54 (3) (2001) 459–468, https://doi.org/10.1016/S0039-9140(00)00544-0.

[107] L. Bernstein, D. Brown, A. Hurst, J. Kelly, F. Kondev, E. McCutchan, C. Nesaraja, R. Slaybaugh, A. Sonzogni, Nuclear Data Needs and Capabilities for Applications, arXiv preprint arXiv:1511.07772..

[108] L.A. Rodríguez Palomino, J. Dawidowski, J.I. Márquez Damián, G.J. Cuello, G. Romanelli, M. Krzystyniak, Neutron total cross-section of hydrogenous and deuterated 1- and 2-propanol and n-butanol measured using the vesuvio spectrometer, Nucl. Instrum. Methods Phys. Res. A 870 (2017) 84–89, https://doi.org/10.1016/j.nima.2017.07.027.

[109] Goran Škoro, Giovanni Romanelli, Svemir Rudić, Steven Lilley, Felix Fernandez-Alonso, Discovery of new neutron-moderating materials at isis neutron and muon source, EPJ Web Conf. 239 (2020) 17008, https://doi.org/10.1051/epjconf/202023917008.

[110] M. Martellucci, G. Romanelli, S. Valeri, D. Cottone, C. Andreani, R. Senesi, The sciences and applications of the electron linac-driven neutron source in Argentina, The European Physical Journal Plusdoi:10.1140/epjp/s13360-021-01243-z..

[111] K. Sakr, W. Ramadan, M. Sayed, T. El-Zakla, M. El-Desouqy, N. El-Faramawy, Utilization of barite/cement composites for gamma rays attenuation, Radiat. Eff. Defect Solid 173 (3–4) (2018) 269–282, https://doi.org/10.1080/10420150.2018.1434520.

[112] I. Akkurt, A. El-Khayatt, The effect of barite proportion on neutron and gamma-ray shielding, Ann. Nucl. Energy 51 (2013) 5–9, https://doi.org/10.1016/j.anucene.2012.08.026.